

Quantum heat engine power can be increased by noise-induced coherence

Marlan O. Scully^{a,b,1}, Kimberly R. Chapin^b, Konstantin E. Dorfman^{a,b}, Moochan Barnabas Kim^b, and Anatoly Svidzinsky^{a,b}

^aPrinceton University, Princeton, NJ 08544; and ^bTexas A&M University, College Station, TX 77843

Contributed by Marlan O. Scully, July 1, 2011 (sent for review June 20, 2011)

Laser and photocell quantum heat engines (QHEs) are powered by thermal light and governed by the laws of quantum thermodynamics. To appreciate the deep connection between quantum mechanics and thermodynamics we need only recall that in 1901 Planck introduced the quantum of action to calculate the entropy of thermal light, and in 1905 Einstein's studies of the entropy of thermal light led him to introduce the photon. Then in 1917, he discovered stimulated emission by using detailed balance arguments. Half a century later, Scovil and Schulz-DuBois applied detailed balance ideas to show that maser photons were produced with Carnot quantum efficiency (see Fig. 1A). Furthermore, Shockley and Quiesser invoked detailed balance to obtain the efficiency of a photocell illuminated by "hot" thermal light (see Fig. 2A). To understand this detailed balance limit, we note that in the QHE, the incident light excites electrons, which can then deliver useful work to a load. However, the efficiency is limited by radiative recombination in which the excited electrons are returned to the ground state. But it has been proven that radiatively induced quantum coherence can break detailed balance and yield lasing without inversion. Here we show that noise-induced coherence enables us to break detailed balance and get more power out of a laser or photocell QHE. Surprisingly, this coherence can be induced by the same noisy (thermal) emission and absorption processes that drive the QHE (see Fig. 3A). Furthermore, this noise-induced coherence can be robust against environmental decoherence.

Quantum mechanics began with the thermodynamic studies of Planck (1) and Einstein (2). In later work Einstein introduced the concept of stimulated emission via the detailed balance arguments (3). After the advent of the maser, Scovil and Schulz-DuBois (4) showed the quantum efficiency for the maser is described by a Carnot relation, and Shockley and Quiesser (5) used detailed balance limit to obtain a similar relation for a photocell. However, in the later part of the twentieth century it was shown that detailed balance could be superseded by using quantum coherence; this is manifested in lasing without inversion (6–8).

Recent studies of a photocell QHE (9) show that it is possible to use microwave induced coherence to break detailed balance and enhance quantum efficiency (i.e., open circuit voltage). But what about enhancing the cell power? It takes energy to generate the microwaves—can we avoid this? A similar question can be asked concerning the laser QHE: Can we use quantum coherence to increase the net emitted laser power? More to the point, can we increase the power output of, for example, a photocell by using noise-induced coherence (10) such as that produced by Fano interference, to break detailed balance? The perhaps surprising (11) answer is yes.*

To answer this question, let us consider the case in which the lowest level is replaced by the pair of levels as in Fig. 1C. Now the plot thickens. In addition to producing a population inversion, the hot and cold photons can induce coherence between levels b_1 and b_2 ; where the amount of coherence is determined by the off diagonal matrix elements (12, 13) $\rho_{b_1, b_2} = \rho_{12}$ given in Eq. 3. We find that this coherence can markedly enhance the power [see also Fleischhauer et al. (14, 15) and Kozlov et al. (16)].

The coherence induced by the hot and cold thermal radiation can be obtained from the density matrix equations of motion

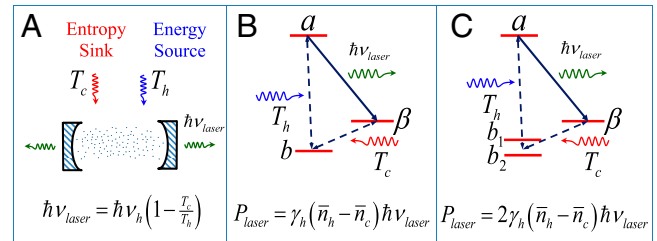


Fig. 1. (A) Schematic of a laser pumped by hot photons at temperature T_h (energy source, blue) and by cold photons at temperature T_c (entropy sink, red). The laser emits photons (green) such that at threshold the laser photon energy and pump photon energy is related by Carnot efficiency (4). (B) Schematic of atoms inside the cavity. Lower level b is coupled to the excited states a and β . The laser power is governed by the average number of hot and cold thermal photons, \bar{n}_h and \bar{n}_c . (C) Same as B but lower b level is replaced by two states b_1 and b_2 , which can double the power when there is coherence between the levels.

(see Appendix). To understand the physical origin of the noise-induced coherence we consider the probability ρ_{11} of being in the state b_1 , which obeys the following equation of motion with physical interpretation depicted on the next line:

$$\begin{aligned} \dot{\rho}_{11} = & \gamma_{1c}[(1 + \bar{n}_c)\rho_{\beta\beta} - \bar{n}_c\rho_{11}] + \gamma_{1h}[(1 + \bar{n}_h)\rho_{aa} - \bar{n}_h\rho_{11}] \\ & - (\gamma_{12c}\bar{n}_c + \gamma_{12h}\bar{n}_h)Re[\rho_{12}] \\ = & \begin{array}{c} \text{---} a \\ \text{---} \beta \\ \text{---} b_1 \quad b_2 \end{array} + \begin{array}{c} \text{---} a \\ \text{---} \beta \\ \text{---} b_1 \quad b_2 \end{array} + \begin{array}{c} \text{---} a \\ \text{---} \beta \\ \text{---} b_1 \quad b_2 \end{array} + \begin{array}{c} \text{---} a \\ \text{---} \beta \\ \text{---} b_1 \quad b_2 \end{array} \end{aligned} \quad [1]$$

Here $\gamma_{kc}(\gamma_{kh})$, $k = 1, 2$, is the spontaneous emission rate of the $\beta \rightarrow b_k$ ($a \rightarrow b_k$) transition, $\gamma_{12c}(\gamma_{12h})$ are cross-coupling coefficients that describe the effect of interference[†], \bar{n}_h and \bar{n}_c are average number of hot and cold thermal photons (17) given by the Planck factors $\bar{n}_c = (\exp[(E_a - E_b)/kT_c] - 1)^{-1}$, $\bar{n}_h = (\exp[(E_\beta - E_b)/kT_h] - 1)^{-1}$.

The power generated by the laser is

$$\frac{P_l}{\hbar\nu_l} = \frac{g^2}{\gamma_l}(\rho_{aa} - \rho_{\beta\beta})\bar{n}_l, \quad [2]$$

Author contributions: M.O.S. conceived the project, carried out the first calculations, and wrote the first draft of the paper; M.O.S., K.E.D., and A.S. designed the research; M.O.S., K.R.C., K.E.D., M.B.K., and A.S. performed the research; M.O.S. and A.S. designed new analytical tools; A.S. showed that the coherence can be robust; and M.O.S., K.R.C., K.E.D., and M.B.K. wrote the paper.

The authors declare no conflict of interest.

*At least it seems to surprise Kirk (11), who says incorrectly: "As Harris shows in his 1989 work on lasing without inversion, Fano interference does not break detailed balance."

We disagree, as does Harris, and we thank him for allowing us to so report. Quantum noise-induced coherence can indeed increase power output, as clearly shown in Fig. 3.

[†]Full coherence $\gamma_{12h} = \sqrt{\gamma_{1h}\gamma_{2h}}$ and $\gamma_{12c} = \sqrt{\gamma_{1c}\gamma_{2c}}$; partial coherence $\gamma_{12h} = 0$ and $\gamma_{12c} = \sqrt{\gamma_{1c}\gamma_{2c}}$; no coherence $\gamma_{12h} = \gamma_{12c} = 0$.

[‡]To whom correspondence should be addressed. E-mail: scully@tamu.edu.

This article contains supporting information online at www.pnas.org/lookup/suppl/doi:10.1073/pnas.1110234108/-DCSupplemental.

where \bar{n}_l is the average number of laser photons, g is atom-field coupling constant, and γ_l is the spontaneous decay rate at the lasing transition $a \rightarrow \beta$.

Thus, as discussed in *Appendix* and in *SI Text*, we solve the density matrix equations for populations ρ_{aa} and $\rho_{\beta\beta}$ as well as quantum coherence ρ_{12} in steady state. For $\gamma_{1h} = \gamma_{2h} = \gamma_h$, $\gamma_{1c} = \gamma_{2c} = \gamma_c$ the maximum coherence and laser power (18) are given by

$$\rho_{12} = \frac{P_l}{4\gamma_h \bar{n}_h \hbar \nu_l}, \quad P_l = A(\bar{n}_h - \bar{n}_c) \hbar \nu_l, \quad [3]$$

where rate A is a function of decay rates γ_c and γ_h and the Planck average photon numbers \bar{n}_h , \bar{n}_c (see *Appendix* and *SI Text*). For the appropriate choice of parameters[‡], $A = \gamma_h$ for the system with no coherence and $A = 2\gamma_h$ with coherence—i.e., the power can be doubled (18), as in Fig. 1. Furthermore, Figs. 1 and 3 show that laser power can be significantly enhanced in the presence of coherence in general. Physically this is because the coherence can lead to faster removal of atoms from the ground state $b_{1,2}$ to the upper laser level a increasing useful work. That is, quantum coherence and interference enhances absorption of solar photons; because the $\tilde{\gamma}_{12}$ terms result in redistribution of the population between b_1 and b_2 states such that the state with stronger coupling to the upper level a becomes more populated. This increases the number of absorbed photons and the current through the cell. Such interference can enhance photon absorption as in the present model or suppress it, which is the case for lasing without inversion.

Next we consider the photocell QHE of Fig. 2 and study the influence of quantum interference and coherence on PV operation (i.e., power generated). Here we will consider a narrow band of frequencies as in the case of a multiplex array of photocells. That is, to optimally utilize a broad solar spectrum one can divide the incident solar flux into narrow frequency intervals, each of which is directed to a quantum dot photocell with its energy spacing matched to the incident light. Monochromatic solar radiation excites electrons from the valence to conduction states in the quantum dots. The “built-in” field in the depletion layer separates electrons and holes; however, they can radiatively recombine before being separated. In the complete analysis (see *SI Text*) we consider the general coupling associated with emission and absorption of solar photons and thermal phonons. This requires a little more elaborate density matrix treatment but the physics is essentially the same as the preceding laser problem. Furthermore, we here focus on the power generated, not the open circuit voltage, as is the case in ref. 9. However, the issue of breaking detailed balance in a photocell via quantum coherence remains the essence of the problem.

In the photocell model (19, 20) of Fig. 2 *B* and *C* the cell current j and voltage V between levels α and β are given by (see *Appendix*)

$$j = e\Gamma\rho_{\alpha\alpha} \quad \text{and} \quad eV = E_\alpha - E_\beta + kT_c \ln\left(\frac{\rho_{\alpha\alpha}}{\rho_{\beta\beta}}\right), \quad [4]$$

where Γ is the decay of level α and ρ_{ii} ($i = \alpha, \beta$) are the occupation probabilities of states in the conduction and lower energy valence reservoirs having energies E_α and E_β . If levels b_1 and b_2 are degenerate and $\gamma_{1h} = \gamma_{2h} = \gamma_h$ the quantum coherence and power $= jV$ are found to be

[‡]In the strong pump limit, $\bar{n}_h \gg 1$, $\bar{n}_c \ll 1$, $\gamma_h \bar{n}_h \ll \gamma_c \gamma_l$, the laser power is given by the simple expression shown in Fig. 1 *B* and *C* where γ_h is the radiative decay rate from $a \rightarrow b$ and hot and cold photon Planck factors \bar{n}_h , \bar{n}_c are discussed in the text.

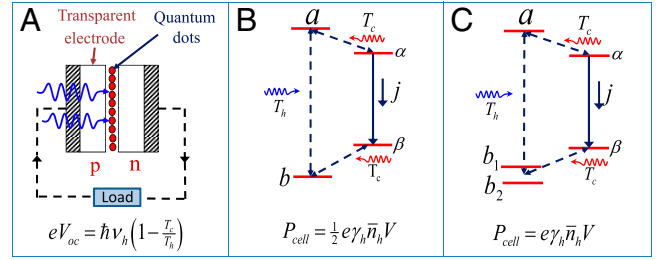


Fig. 2. (A) Schematic of a photocell consisting of quantum dots sandwiched between p and n doped semiconductors. Open circuit voltage and solar photon energy $\hbar\nu_h$ are related by the Carnot efficiency factor where T_c is the ambient and T_h is the solar temperature. (B) Schematic of a quantum dot solar cell in which state b is coupled to a via, e.g., solar radiation and coupled to the valence band reservoir state β via optical phonons. The electrons in conduction band reservoir state α pass to state β via an external circuit, which contains the load. (C) Same as *B* but lower level b is replaced by two states b_1 and b_2 , and when coherently prepared can double the output power.

$$\rho_{12} = \frac{j}{4e\gamma_h \bar{n}_h}, \quad P_{\text{cell}} = eB\bar{n}_h V \quad [5]$$

which is similar to Eq. 3 for the laser QHE in which the laser photon flux $P_l/\hbar\nu_l$ is now replaced by the photocell current. Factor B is similar to A and for the appropriate choice of parameters[§] $B = \gamma_h/2$ for the system with singlet shown in Fig. 2*B*, $B = 2\gamma_h/3$ for the doublet model (Fig. 2*C*), and no coherence and $B = \gamma_h$ with full coherence—i.e., the photocell QHE power can be doubled by quantum coherence just as in the case of the laser.

Fig. 3*A* shows the photocell current j (photon flux $P_l/\hbar\nu_l$) as a function of voltage (energy) of the electrons (laser photons). We find that the induced coherence substantially increases the cell current (photon flux) and therefore the power of the QHE. As in the laser QHE, quantum coherence in the photocell QHE results in the faster removal of electrons from the recombination region, so that we can reduce the $a \rightarrow b_{1,2}$ transition and enhance the photocurrent $\alpha \rightarrow \beta$. This reduces recombination losses and increases the power delivered to the load. For example, in the limit of a weak pump, $\bar{n}_h \ll 1$, appropriate for a photodetector, the signal power is doubled by quantum coherence[¶] (see Fig. 2*B* and *C*).

It is important to note that effects of environmentally induced decoherence τ_2 on photocell power can be made small by proper cell design. For the typical case in which the phonon occupation number \bar{n}_c is large, Eq. 8 shows that the stimulated phonon absorption $(\gamma_{1c} + \gamma_{2c})\bar{n}_c$ term dominates other possible decoherence channels (τ_2 effects) even when the environmental effect is substantial $\frac{1}{\tau_2} \gg \gamma_{1,2c}$. As a result, one can have a photocell with PV characteristics shown in Fig. 3*B* such that the noised induced quantum coherence is robust against environmental decoherence.^{||}

To summarize: There exists a close analogy between the laser QHE pumped by hot photons and cooled by a lower temperature entropy sink and a photocell QHE that is driven by hot photons while the ambient heat reservoir serves as the lower temperature entropy sink (21). Furthermore, we have shown that quantum

[§]For instance if $\bar{n}_c \gg 1$, $\bar{n}_h \ll 1$, $\gamma_h \ll \gamma_c \bar{n}_c$.

[¶]In this case the maximum current $j = e\gamma_h \bar{n}_h$ is to be compared with the current generated by incoherent doublet $\frac{2}{3}e\gamma_h \bar{n}_h$ and $\frac{1}{2}e\gamma_h \bar{n}_h$ for a single lower level as per Fig. 2*B*. As per Fig. 3*A* simulation we take $T_h = 0.5$ eV, $T_c = 0.0259$ eV, $E_a - E_b = 1.43$ eV, $E_\beta - E_b = 0.005$ eV, $\gamma_{2h} = 0.1\gamma_{1h}$, $\gamma_{1c} = 50\gamma_{1h}$, $\gamma_{2c} = 5.5\gamma_{1h}$. In addition for a photocell QHE $E_a - E_\alpha = 0.005$ eV and $\gamma_{a \rightarrow \alpha} = 50\gamma_1$.

^{||}As an illustration we consider a model in which levels b_1 and b_2 are degenerate and take $T_h = 0.5$ eV, $T_c = 0.0259$ eV, $E_a - E_\alpha = E_\beta - E_b = 0.0002$ eV, $E_a - E_\beta = 1.4296$ eV, $\gamma_{2h} = 0.01\gamma_{1h}$, $\gamma_{1c} = 50\gamma_{1h}$, $\gamma_{2c} = 10^{-5}\gamma_{1h}$, and $\gamma_{a \rightarrow \alpha} = 50\gamma_1$.

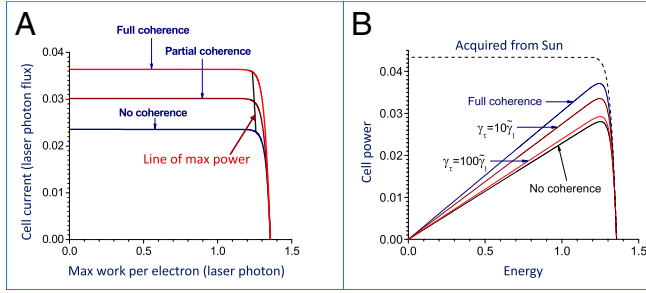


Fig. 3. (A) Photocell current $j = \Gamma\rho_{\alpha\alpha}$ (laser photon flux $P_l/h\nu_l$) (in arbitrary units) generated by the photovoltaic cell QHE (laser QHE) of Fig. 1C (Fig. 2C) as a function of maximum work (in electron volts) done by electron (laser photon) $E_\alpha - E_\beta + kT_c \log(\rho_{\alpha\alpha}/\rho_{\beta\beta})$ with full (red line), partial (brown line), and no quantum interference (blue line). (B) Power of a photocell of Fig. 2C as a function of voltage for different decoherence rates $\gamma_\tau \equiv \frac{1}{2} = 10\gamma_{1c}, 100\gamma_{1c}$. Upper curve indicates power acquired from the sun.

interference can enhance laser and PV thermodynamic power beyond the limit of a system, which does not possess quantum coherence. Moreover, coherence generated by noise-induced quantum interference is essentially different from the quantum coherence produced by an external microwave field (9), which costs energy. In the present paper, quantum coherence is generated by the photocurrent due to quantum interference. No additional energy source is necessary to create such induced coherence. Nevertheless, as we have shown, the induced coherence can, in principle, enhance the efficiency of photovoltaic devices such as solar cells and/or photodetectors. We note that in the case of solar cells, the power generated** is always less than the incident power times the Carnot factor—i.e., $P < P_{\text{solar}}(1 - \frac{T_c}{T_s})$. In the case of photodetector operating at low temperature the phase coherence time T_2 can be relatively long, and applications of the present work to photodetection near at hand. Practical application to solar cell systems is possible but requires further research. However it is clear that the ultimate “in principle” limit of such devices is an important question of fundamental interest.

Appendix

Here we give (see *SI Text* for more detail) the density matrix equations for a laser QHE model of Fig. 1C. Radiation coming from a heat bath at temperature T_h drives transitions from b_1 and b_2 to a . Entropy sink couples b_1 and b_2 to level β via emission of thermal photons at temperature T_c . Levels a and β correspond to lasing transition. For degenerate lower levels b_1 and b_2 the evolution of density matrix elements $\rho_{ik} \stackrel{\text{def}}{=} \rho_{b_i b_k}$ given by

$$\dot{\rho}_{11} = \gamma_{1c}[(1 + \bar{n}_c)\rho_{\beta\beta} - \bar{n}_c\rho_{11}] + \gamma_{1h}[(1 + \bar{n}_h)\rho_{aa} - \bar{n}_h\rho_{11}] - (\gamma_{12c}\bar{n}_c + \gamma_{12h}\bar{n}_h)\text{Re}[\rho_{12}], \quad [6]$$

$$\dot{\rho}_{22} = \gamma_{2c}[(1 + \bar{n}_c)\rho_{\beta\beta} - \bar{n}_c\rho_{22}] + \gamma_{2h}[(1 + \bar{n}_h)\rho_{aa} - \bar{n}_h\rho_{22}] - (\gamma_{12c}\bar{n}_c + \gamma_{12h}\bar{n}_h)\text{Re}[\rho_{12}], \quad [7]$$

**In the present paper, as in ref. 9, we are always in complete accord with the laws of thermodynamics; this is in contrast with statements found in ref. 11, wherein Kirk states incorrectly that ref. 9 seems to have “identified a PV cell that can now generate more power than that which is radiated from the sun.” This is an incorrect statement for various reasons—for example, the open circuit voltage, not the power, is determined in ref. 9. Furthermore, the calculated power given in the present paper is always less than that radiated from the sun (see Fig. 3B).

$$\dot{\rho}_{12} = -\frac{1}{2}[(\gamma_{1h} + \gamma_{2h})\bar{n}_h + (\gamma_{1c} + \gamma_{2c})\bar{n}_c]\rho_{12} - \frac{\rho_{12}}{\tau_2} + \gamma_{12h}\left[(1 + \bar{n}_h)\rho_{aa} - \frac{1}{2}\bar{n}_h(\rho_{11} + \rho_{22})\right] + \gamma_{12c}\left[(1 + \bar{n}_c)\rho_{\beta\beta} - \frac{1}{2}\bar{n}_c(\rho_{11} + \rho_{22})\right] \quad [8]$$

$$\dot{\rho}_{\beta\beta} = \gamma_{1c}[\bar{n}_c\rho_{11} - (1 + \bar{n}_c)\rho_{\beta\beta}] + \gamma_{2c}[\bar{n}_c\rho_{22} - (1 + \bar{n}_c)\rho_{\beta\beta}] + 2\gamma_{12c}\bar{n}_c\text{Re}[\rho_{12}] + \frac{P_l}{h\nu_l}, \quad [9]$$

$$\rho_{11} + \rho_{22} + \rho_{aa} + \rho_{\beta\beta} = 1, \quad [10]$$

where for maximum quantum interference $\gamma_{12h} = \sqrt{\gamma_{1h}\gamma_{2h}}$, $\gamma_{12c} = \sqrt{\gamma_{1c}\gamma_{2c}}$, while for no coherence $\gamma_{12h} = \gamma_{12c} = 0$. The laser power as determined by the net emission rate between a and β is

$$\frac{P_l}{h\nu_l} \equiv \frac{g^2}{\gamma_l}[(\bar{n}_l + 1)\rho_{aa} - \bar{n}_l\rho_{\beta\beta}], \quad [11]$$

which yields Eq. 2 when $\bar{n}_l \gg 1$. We focus on steady state operation. In this regime, one can easily solve Eqs. 6–10 and obtain populations and coherence ρ_{12} .

The photocell of Fig. 2C is very similar in spirit and mathematics to the laser QHE of Fig. 1C. However, there are a few differences. For example, the electron charge times the voltage (eV) in the photocell is replaced by $h\nu_l$ in the laser. To get a simple solution for the voltage, one can simply introduce the Fermi Dirac distribution for two arbitrary levels α and β

$$\rho_{\alpha\alpha} = P_\alpha = \frac{1}{\exp(\frac{E_\alpha - \mu_\alpha}{kT}) + 1}, \quad \rho_{\beta\beta} = P_\beta = \frac{1}{\exp(\frac{E_\beta - \mu_\beta}{kT}) + 1}. \quad [12]$$

In the high temperature limit for the quantum photocell we obtain

$$eV = \mu_\alpha - \mu_\beta = E_\alpha - E_\beta + kT \ln\left(\frac{P_\alpha}{P_\beta}\right). \quad [13]$$

Another difference between the laser and photocell is the introduction of conduction band reservoir level α as in Fig. 2B and C; and the identification of the current $j = e\Gamma\rho_{\alpha\alpha}$, which does not apply for the case of the laser. To determine the laser power, we use Eq. 11. The correspondence between the laser QHE and the photocell QHE is striking and useful.

ACKNOWLEDGMENTS. It is a pleasure to thank our esteemed colleague George Kattawar for many enlightening discussions on optics, physics, and more. We also gratefully acknowledge support for this work by National Science Foundation Grant EEC-0540832 (MIRTHE ERC), the Office of Naval Research, and the Robert A. Welch Foundation (A-1261).

- Planck M (1901) On the law of distribution of energy in the normal spectrum. *Ann Phys* 309:553.
- Einstein A (1905) On a heuristic viewpoint concerning the production and transformation of light. *Ann Phys* 322:132–148.
- Einstein A (1917) On the quantum mechanics of radiation. *Physik Zeitschr* 18:121–128.
- Scovil HED, Schulz-DuBois EO (1959) Three-level masers as heat engines. *Phys Rev Lett* 2:262–263.
- Shockley W, Queisser HJ (1961) Detailed balance limit of efficiency of p-n junction solar cells. *J Appl Physiol* 32:510–519.

6. Kocharovskaya OA (1992) Amplification and lasing without inversion. *Phys Rep* 219:175–190.
7. Harris SE (1997) Electromagnetically induced transparency. *Phys Today* 50:36–42.
8. Scully MO, Zubairy MS (1997) *Quantum Optics* (Cambridge Univ Press, Cambridge, UK).
9. Scully MO (2010) Quantum photocell: Using quantum coherence to reduce radiative recombination and increase efficiency. *Phys Rev Lett* 104:207701.
10. Agarwal G (1974) *Quantum Statistical Theories of Spontaneous Emission and Their Relation to other Approaches*, Springer Tracts in Modern Physics (Springer, Berlin), 70.
11. Kirk AP (2011) Analysis of quantum coherent semiconductor quantum dot p-i-n junction photovoltaic cells. *Phys Rev Lett* 106:048703.
12. Friedrich B, Herschbach D (1996) Statistical mechanics of pendular molecules. *Int Rev Phys Chem* 15:325–344.
13. Schleich WP (2001) *Quantum Optics in Phase Space* (Wiley-VCH, Berlin).
14. Fleischhauer M, Keitel CH, Scully MO, Su C (1992) Lasing without inversion and enhancement of the index of refraction via interference of incoherent pump processes. *Opt Commun* 87:109–114.
15. Fleischhauer M, McIllrath M, Scully MO (1995) Coherent population trapping and fano-type interferences in lasing without inversion. *Appl Phys B* 60:S123–S127.
16. Kozlov VV, Rostovtsev Y, Scully MO (2006) Inducing quantum coherence via decays and incoherent pumping with application to population trapping, lasing without inversion, and quenching of spontaneous emission. *Phys Rev A* 74:063829.
17. Lee MH (2001) Carnot cycle for photon gas? *Am J Phys* 69:874–878.
18. Boukobza E, Tannor D (2007) Three-level systems as amplifiers and attenuators: A thermodynamic analysis. *Phys Rev Lett* 98:240601.
19. Faist J, et al. (1997) Controlling the sign of quantum interference by tunneling from quantum wells. *Nature* 390:589–591.
20. Nikonov DE, Immamoglu A, Scully MO (1999) Fano interference of collective excitations in semiconductor quantum wells and lasing without inversion. *Phys Rev B Condens Matter Mater Phys* 59:12212–12125.
21. Scully M (2011) Comment on Analysis of quantum coherent semiconductor quantum dot p-i-n junction photovoltaic cells. *Phys Rev Lett* 106:049801.